

Quantum Lifshitz Point

R. Ramazashvili

*Loomis Laboratory, University of Illinois at Urbana-Champaign,
Urbana, IL 61801-3080, USA.*

Abstract

I study a quantum Lifshitz point in a three-dimensional itinerant antiferromagnet, in particular the scaling of the Néel temperature, the correlation length, the staggered susceptibility, the specific heat coefficient and the resistivity. At low temperatures, the model is shown to have the inverse staggered susceptibility and the resistivity varying as $T^{5/4}$, and the specific heat coefficient varying as $T^{1/4}$.

PACS numbers:

I. INTRODUCTION

Magnetic metals close to a zero temperature phase transition have been a subject of active ongoing study¹, mainly due to their apparent defiance of the Fermi liquid paradigm. Near a quantum critical point, one usually finds neither a nearly constant linear specific heat coefficient $\gamma \equiv \delta C/T \sim \text{const.}$, nor a virtually temperature-independent magnetic susceptibility $\chi \sim \text{const.}$, nor a T^2 -resistivity $\rho \sim \text{const.} + T^2$, all normally expected from a Landau Fermi liquid². Instead experiments reveal a host of anomalous thermodynamic, magnetic and transport properties¹ calling for adequate theoretical description.

In its current form, scaling theory of quantum criticality in itinerant magnets is due to Hertz³ and Millis⁴. It describes incipient magnetic ordering in an isotropic metal solely in terms of a boson order parameter with the correlation range in both space and time diverging at a quantum critical point. This divergence naturally leads to low-temperature anomalies in thermodynamic, magnetic and transport properties. Some of the early work on the subject was done by Mathon⁵, Makoshi and Moriya⁶, Ueda⁷ and Dzyaloshinskii and Kondratenko⁸, who described magnetic transitions at $T = 0$ using diagrammatic methods. These and other studies of nearly ferro- and antiferromagnetic metals as well as magnetic fluctuations in general, done in the spirit of self-consistent theory, were summarized in the book by Moriya⁹. A phenomenological approach aiming at establishing relations between various critical exponents at a quantum critical point has been developed by Continentino¹⁰.

The Hertz-Millis theory and its implications describe rather well some itinerant ferromagnets such as ZrZn_2 and, to a lesser extent, MnSi . In ZrZn_2 , moderate external pressure $p \approx 8$ kbar is enough to reduce the Curie temperature T_C to zero. Near the critical pressure p_c , T_C scales as $(p_c - p)^{3/4}$ while the resistivity obeys^{11,12} $\rho \sim T^{1.6 \pm 0.1}$, in excellent agreement with the theory^{4,5,9}.

At the same time, several Ce-based antiferromagnets, where the Néel temperature can be tuned to zero by pressure or doping, appear to disregard the conclusions of the available theories. One of the most studied examples is¹³ $\text{CeCu}_{6-x}\text{Au}_x$, where at the quantum critical

point the resistivity behaves as $const. + T$, and where over more than two decades in temperature the specific heat coefficient diverges as $\ln(T)$ while the inverse susceptibility fits¹⁴ $\chi^{-1} \sim const. + T^\alpha$ with $\alpha \approx 0.8 \pm 0.1$.

Another interesting case is $CePd_2Si_2$, a metal which orders antiferromagnetically below 10 K. Applied pressure reduces the Néel temperature T_N from 10 K at the ambient pressure to about 0.4 K at 28 kbar. Between 15 kbar and 28 kbar, T_N falls linearly with pressure, and at 28 kbar $CePd_2Si_2$ becomes superconducting below 0.4 K, in a narrow strip between 23 and 32 kbar¹². At 28 kbar, the resistivity of $CePd_2Si_2$ exhibits a striking $T^{1.2 \pm 0.1}$ behavior over about two decades in temperature¹².

Neither $CeCu_{6-x}Au_x$ nor $CePd_2Si_2$ appear to respect the available theoretical results which, for a bulk antiferromagnet, would imply the Néel temperature scaling⁴ as $T_N \sim (p_c - p)^{2/3}$, the specific heat coefficient^{6,9} $\gamma \sim T^{1/2}$ and the resistivity^{7,9} $\rho \sim T^{3/2}$. At the same time, theoretical results for *two* dimensions are much closer to what was observed in $CeCu_{6-x}Au_x$, as in this case the theory does yield $const. + T$ resistivity¹⁵, logarithmically divergent linear specific heat coefficient and essentially linear scaling of the Néel temperature with pressure⁴. This led to an interpretation of data on $CeCu_{6-x}Au_x$ in terms of a purely two-dimensional magnetic ordering in an otherwise perfectly three-dimensional metal with only moderate anisotropy^{15,16}.

An alternative interpretation¹⁴, based on the neutron scattering data, pointed at a possible explanation in terms of highly anisotropic critical fluctuations with the stiffness in one of the directions vanishing at or very close to the quantum critical point. The conspiracy of this anisotropy with the anomalous frequency exponent¹⁴ $\alpha \approx 0.8 \pm 0.1$ of critical fluctuations allowed to fit together the large body of experimental data obtained at the quantum critical point in $CeCu_{6-x}Au_x$, including the specific heat, the uniform susceptibility and the neutron scattering scans.

This latter scenario would imply a residual quartic dispersion ($\sim q^4$) of critical fluctuations in the “soft” direction, thus also leading to the dimensionality reduction (by 1/2, as opposed to the purely two-dimensional order) and hence to qualitative modification of the

Hertz-Millis theory.

Finally, it was noticed^{17,18} that the resistivity $\rho \sim T^{1.2 \pm 0.1}$ of CePd₂Si₂, as well as $\rho \sim T^{1.25 \pm 0.1}$ of CeNi₂Ge₂ (which has the structure of CePd₂Si₂ with a smaller unit cell) may also be explained assuming anisotropic critical fluctuations with the residual quartic dispersion in one of the directions.

All these experimental findings suggest that vanishing stiffness may be the aspect of physics needed to describe the quantum criticality in Ce-based antiferromagnets by a Hertz-Millis type of theory. A critical point which, in addition to the onset of ordering, is characterized by disappearance of stiffness in one or several directions, is called a Lifshitz point¹⁹. In this paper, I study a *quantum* Lifshitz point, a curious yet possibly experimentally relevant coincidence of a *quantum* critical point (onset of ordering at $T = 0$) with a point where the stiffness vanishes in one or several directions in the momentum space. I develop scaling theory of a classical Gaussian region⁴ of a disordered phase near a quantum Lifshitz point in an itinerant three-dimensional magnet. I study a particular case of a Lifshitz point, where the incipient ordering exhibits anisotropic dispersion^{14,17,18} which is quartic in only *one* direction and quadratic in the remaining two.

The restriction to only the classical Gaussian region is due to the fact that in the other regions the low-temperature behavior is dominated by crossovers between various regimes and thus comparison to the experiment is rather hard to make. Moreover, the full phase diagram is sensitive to the relative strength of the coupling constants, whereas the results for the classical Gaussian region of a disordered phase are independent of this uncertainty and can be tested experimentally.

It is important to note that Lifshitz point is a multicritical point and that, generally, one shall expect to find three phases in its vicinity, corresponding to one disordered and two different ordered states (see Section V). At the same time, none of the experiments on CeCu_{6-x}Au_x or CePd₂Si₂ which I am aware of, indicated presence of more than one magnetically ordered phase. To that end, I show that, near a *quantum* Lifshitz point, one may indeed find only *one* ordered phase rather than two, which makes the model potentially

relevant to $\text{CeCu}_{6-x}\text{Au}_x$ ^{13–16}, CePd_2Si_2 and CeNi_2Ge_2 ^{12,17,18,20–22}.

Bearing in mind that both CePd_2Si_2 and $\text{CeCu}_{6-x}\text{Au}_x$ are antiferromagnetic metals, one is led to assume that the critical mode is non-conserved and over-damped. Therefore this work may be viewed as an experiment-motivated extension of the Hertz-Millis theory^{3,4} to a particular case of a quantum Lifshitz point.

In Section II, I present the results and discuss them. I determine the equation of the critical line, the behavior of the order parameter susceptibility and the correlation length close to the quantum Lifshitz point. I also estimate the low-temperature behavior of the conductivity and the anomaly of the linear specific heat coefficient. Then I compare these theoretical results with the experimental findings^{12,16,17,20–22}.

In Section III, I derive the scaling equations, solve them in Section IV and obtain the results outlined in Section II. In Section V, I discuss the phase diagram near the quantum Lifshitz point and set the conditions for appearance of only one ordered phase.

To demonstrate that the quantum Lifshitz point I study is well defined, in Section VI I examine how interactions generate stiffness in the “soft” direction, and show that this effect can be neglected at all relevant momenta and frequencies. Finally, in Section VII, I summarize the results and comment on them. The appendix provides the calculation details.

Self-consistent treatment of a model with the stiffness vanishing in one of the directions in the momentum space has been given recently by C. Lacroix *et al.*²³ with reference to the experimental data²⁴ on YMn_2 -based materials, where the transition is *first-order*. The present work amounts to a renormalization group derivation of some of the results obtained in²³ (staggered susceptibility), plus new results (specific heat coefficient, possible phase diagrams and the transition line equation) along with comparison to the experimental data for Ce-based metallic antiferromagnets undergoing second-order phase transition. It is also shown that generation of stiffness in the “soft” direction by short-distance fluctuations is negligible at all relevant momenta, and thus the quantum Lifshitz point studied in this paper is well-defined.

II. THE RESULTS

The main results of this Section amount to establishing the leading low-temperature behavior of various quantities near a quantum Lifshitz point. This task is facilitated by the fact that the theory falls above its upper critical dimension. Moreover, since the stiffness in the “soft” direction, generated by the short-range fluctuations, turns out to be negligible (see Section VI), the thermodynamic and transport properties in the classical Gaussian region ($T_N = 0$) may be obtained from the Gaussian action with this stiffness set equal to zero:

$$S[\phi] = \int_0^\beta d\tau \int dx \phi_\alpha \left[\delta + |\partial_\tau| + \nabla_\parallel^2 + \nabla_\perp^4 \right] \phi_\alpha, \quad (1)$$

where δ is defined by the tuning parameter p and by the feedback of the quartic interaction in the Ginzburg-Landau action (2-4) as per $\delta = (p - p_c)/p_c + \text{const.}T^{5/4}$. Thus the Néel temperature T_N in this theory scales as $T_N \sim (p_c - p)^{4/5}$. At $p = p_c$, the correlation length ξ_\parallel scales as $T^{-5/8}$, whereas the correlation length ξ_\perp in the “soft” direction scales as $T^{-5/16}$.

The leading exponent of the specific heat coefficient is given by the Gaussian contribution to the free energy F :

$$F = Tr \log G^{-1}(q, \omega) = \int^1 dz \int^1 d^2 q_\parallel \int^1 dq_\perp \coth \frac{z}{2T} \arctan \left[\frac{z}{q_\parallel^2 + q_\perp^4} \right]$$

and yields the specific heat coefficient

$$\delta C/T \sim T^{1/4}.$$

Resistivity due to scattering off anisotropic fluctuations can be estimated via the characteristic transport time τ_{tr} given by the fluctuations of the magnetic order parameter near the transition. Since the critical fluctuations are antiferromagnetic and thus characterized by a finite wave-vector, the $(1 - \cos \theta)$ factor in the transport relaxation rate may be omitted in a qualitative estimate, which leads to

$$1/\tau_{tr} \sim T \sum_{q, \omega} \langle \phi^2 \rangle_{q, \omega} \sim T^{5/4},$$

as realized indeed by the authors of^{17,18}. Recently, it has been argued²⁵ that the observed resistivity $\rho(T) \sim \text{const.} + T^{1.2 \pm 0.1}$ may be a crossover phenomenon due to the interference between the impurity scattering and scattering by the critical fluctuations, conspiring to mimic a power-law behavior. At the moment it remains to be seen how sensitive this mechanism may be to the material-dependent factors such as the shape of the Fermi surface. At the same time, for a system with a true quantum Lifshitz point, the $T^{5/4}$ resistivity shall be accompanied by the $C/T \sim T^{1/4}$ scaling of the specific heat coefficient.

In CePd₂Si₂ and CeNi₂Ge₂, the resistivity does exhibit^{12,17} a temperature exponent close to 5/4. However, the rest of the available data is less encouraging for the present theory. The Néel temperature scales linearly with pressure¹² instead of obeying $T_N \sim (p_c - p)^{4/5}$. To my knowledge, the specific heat data on CePd₂Si₂ at the critical pressure is not yet available. The specific heat data on CeNi₂Ge₂ is still ambiguous, as both the $C/T \sim T^{1/2}$ and $C/T \sim \log T$ have been reported^{20,22}.

One can indeed find formal reasons (such as presence of the superconducting phase in CePd₂Si₂, or disorder in CeCu_{5.9}Au_{0.1}) why the Lifshitz point theory is not applicable to these materials. However, the $T^{1.2}$ scaling of the resistivity in CePd₂Si₂ is seen at temperatures up to 60 K, which is more than two orders of magnitude greater than the superconducting transition temperature $T_c \approx 0.4$ K. At the same time, virtually linear scaling of T_N with pressure persists up to about 5 K, which is again much greater than T_c . These arguments (as well as recent finding¹⁴ of the ω/T scaling and the inverse *uniform* susceptibility behaving as $\chi^{-1} \sim \text{const.} + T^{0.8 \pm 0.1}$ in CeCu_{5.9}Au_{0.1}) strongly suggest that the physics of these materials amounts to more than just a refined Gaussian theory above its upper critical dimension.

III. THE SCALING EQUATIONS

The assumption of an overdamped critical mode with the stiffness vanishing in one of the directions leads to the following effective action close to the quantum Lifshitz point:

$$S_{eff}[\phi] = S^{(2)} + S^{(4)} \quad (2)$$

$$S^{(2)} = \int_0^\beta d\tau \int dx \phi_\alpha \left[\delta + |\partial_\tau| + \nabla_\parallel^2 + D\nabla_\perp^2 + \nabla_\perp^4 \right] \phi_\alpha \quad (3)$$

$$S^{(4)} = \int_0^\beta d\tau \int dx \left[u(\phi_\alpha \phi_\alpha)^2 + v_1(\nabla_\perp \phi_\alpha)^2 \phi_\beta \phi_\beta + v_2(\phi_\alpha \nabla_\perp \phi_\alpha)^2 \right]. \quad (4)$$

with the frequency and the momentum cut-off set equal to unity. Here the mass term δ and the stiffness D in the “soft” direction describe deviation from the quantum Lifshitz point, $\beta = 1/T$ is the inverse temperature, ∇_\parallel corresponds to the two “normal” directions, whereas ∇_\perp corresponds to the third, “soft” direction. The coupling constants v_1 and v_2 describe the dispersion of the quartic coupling constant u ; they correspond to the only two possible linearly independent terms quadratic in ∇_\perp and quartic in ϕ_α , and describe generation of stiffness in the “soft” direction, as shown in Fig. 3.

The scaling variables in the theory are the mass term δ , the stiffness D in the “soft” direction, the temperature T and coupling constants u , v_1 and v_2 . To the lowest order in the latter three, the scaling equations can be derived e.g. by expanding the partition function Z to first order in $S^{(4)}$, then integrating out a thin shell near the cut-off, rescaling the variables and the fields, and then comparing the result with the original action⁴:

$$\frac{dT(b)}{d \ln b} = 2T(b) \quad (5)$$

$$\frac{du(b)}{d \ln b} = -\frac{1}{2}u(b) \quad (6)$$

$$\frac{dv_{1,2}(b)}{d \ln b} = -\frac{3}{2}v_{1,2}(b) \quad (7)$$

$$\begin{aligned} \frac{d\delta(b)}{d \ln b} &= 2\delta(b) + 2(n+2)u f_1[T(b), \delta(b), D(b)] \\ &\quad + (nv_1 + v_2) f_2[T(b), \delta(b), D(b)] \end{aligned} \quad (8)$$

$$\frac{dD(b)}{d \ln b} = D(b) + (nv_1 + v_2) f_1[T(b), \delta(b), D(b)]. \quad (9)$$

Here n is the number of components of field ϕ_α . The definitions of $f_1[T(b), \delta(b), D(b)]$ and $f_2[T(b), \delta(b), D(b)]$, as well as the details of the derivation, are given in the Appendix. Note that, following Millis⁴, I denote the running value of a scaling variable (e.g. $T(b)$) by indicating explicit dependence on the rescaling parameter b , whereas for the bare (physical)

quantities the b dependence is omitted. Also note that truncating the equations at the first order in u , v_1 and v_2 is equivalent to the assumption that the bare value of these couplings is small.

An extra scaling variable $D(b)$ in equations (5-9) compared with those of Millis⁴ leads to appearance of *two* different ordered phases to be described in Section V. This sets the main distinction between a quantum Lifshitz point and a simple quantum critical point of Hertz and Millis, where there is only one ordered phase.

IV. SOLUTION OF THE SCALING EQUATIONS

In this Section, I obtain the qualitative solution of the scaling equations (5-9) following Millis⁴ and noticing that $f_1[T(b), \delta(b), D(b)]$ and $f_2[T(b), \delta(b), D(b)]$ virtually do not depend on $\delta(b)$ or $D(b)$ for $\delta(b), D(b) \ll 1$, and that both of them fall off rapidly as $\delta(b)$ exceeds unity. Thus one can neglect their dependence on $\delta(b)$ and $D(b)$ for $\delta(b) < 1$ and stop the scaling at $\delta(b) = 1$.

With these provisos, the formal solution of (5-9) reads

$$T(b) = Tb^2 \tag{10}$$

$$u(b) = ub^{-1/2} \tag{11}$$

$$v_{1,2}(b) = v_{1,2}b^{-3/2} \tag{12}$$

$$\begin{aligned} \delta(b) = & \delta b^2 + 2b^2(n+2)u \int_0^{\ln b} d\tau e^{-\frac{5}{2}\tau} f_1[Te^{2\tau}] \\ & + b^2(nv_1 + v_2) \int_0^{\ln b} d\tau e^{-\frac{7}{2}\tau} f_2[Te^{2\tau}] \end{aligned} \tag{13}$$

$$D(b) = b \left[D + (nv_1 + v_2) \int_0^{\ln b} d\tau e^{-\frac{5}{2}\tau} f_1[Te^{2\tau}] \right]. \tag{14}$$

As in the case of a simple quantum critical point⁴, two major regimes exist, depending on whether the scaling stops when the running value of the temperature is much smaller or much greater than one. The first case is usually referred to as quantum while the second case is called classical.

To obtain the condition for the quantum regime, set $T = 0$ on the right hand side of (13), then integrate over τ up to $\ln(b^*)$ such that $\delta(b^*) = 1$, solve for b^* , substitute b^* into (10) and require $T(b^*) \ll 1$. The resulting condition is

$$T \ll r_1, \quad r_1 \equiv \frac{4}{5}(n+2)uf_1[0] + \frac{2}{7}(nv_1 + v_2)f_2[0]. \quad (15)$$

If reversed, the inequality (15) corresponds to the classical regime, where it is convenient to divide the scaling trajectory into two parts, corresponding to $T(b) \ll 1$ (quantum) and $T(b) \gg 1$ (classical). For $T(b) \gg 1$, one can estimate $f_{1,2}[T]$ as $f_1[T] \approx B_1T$, $f_2[T] \approx B_2T$. Then, for $T(b) \gg 1$, the equations (6-9) may be recast in terms of new variables $U(b) \equiv u(b)T(b)$, $V_{1,2}(b) \equiv v_{1,2}(b)T(b)$:

$$\frac{dT(b)}{d \ln b} = 2T(b) \quad (16)$$

$$\frac{dU(b)}{d \ln b} = \frac{3}{2}U(b) \quad (17)$$

$$\frac{dV_{1,2}(b)}{d \ln b} = \frac{1}{2}V_{1,2}(b) \quad (18)$$

$$\frac{d\delta(b)}{d \ln b} = 2\delta(b) + 2B_1(n+2)U(b) + B_2(nV_1(b) + V_2(b)) \quad (19)$$

$$\frac{dD(b)}{d \ln b} = D(b) + B_1(nV_1(b) + V_2(b)). \quad (20)$$

The initial conditions correspond to $b = \bar{b}$ such that $T(\bar{b}) = 1$ and read

$$T(\bar{b}) = 1 \quad (21)$$

$$U(\bar{b}) = u(\bar{b}) = uT^{1/4} \quad (22)$$

$$V_{1,2}(\bar{b}) = v_{1,2}T^{3/4} \quad (23)$$

$$\delta(\bar{b}) = \frac{1}{T} \left[r_1 + A(n+2)uT^{5/4} \right] \quad (24)$$

$$D(\bar{b}) = \frac{1}{\sqrt{T}} \left[r_2 + \frac{A}{2}(nv_1 + v_2)T^{5/4} \right], \quad (25)$$

where r_2 is defined by

$$r_2 \equiv D + \frac{2}{5}(nv_1 + v_2)f_1[0]. \quad (26)$$

For $T \gg r_1$, both $U(\bar{b})$ and $V_{1,2}(\bar{b})$ are small, which justifies using linearized equations near $b = \bar{b}$. Neglecting the higher powers of T and assuming that u and $v_{1,2}$ are of the same order of magnitude, the solution of (16-20) is

$$T(b) = T(\bar{b})b^2 \quad (27)$$

$$U(b) = U(\bar{b})b^{3/2} \quad (28)$$

$$V_{1,2}(b) = V_{1,2}(\bar{b})b^{1/2} \quad (29)$$

$$\delta(b) = b^2 [\delta(\bar{b}) + 4B_1 u(n+2)T^{1/4}] \quad (30)$$

$$D(b) = b [D(\bar{b}) + 2B_1(nv_1 + v_2)T^{3/4}]. \quad (31)$$

Now one can ensure the consistency of using the linearized equations by demanding that, when scaling stops at $\delta(b^*) = 1$, the coupling constant U is small:

$$U(b^*) \ll 1. \quad (32)$$

This condition corresponds to the Ginzburg criterion²⁶ and is violated only very close to the line $\delta(b^*) = 0$, which defines the Néel temperature T_N as a function of u and r_1 :

$$r_1 + (A + 4B_1)(n+2)uT_c^{5/4} = 0. \quad (33)$$

The Ginzburg criterion (32) is violated in a narrow window $\delta T_N/T_N \sim u^{1/3}T_c^{1/12} \ll 1$ of strong classical fluctuations.

To establish connection with experiment, it is assumed that r_1 and r_2 are both proportional to the deviation $(p - p_c)$ of the control parameter p from its critical value p_c . This is a reasonable assumption given that the theory at hand is above the upper critical dimension. Thus T_N scales as per

$$T_N \sim (p_c - p)^{4/5}. \quad (34)$$

However, which two phases does the line (34) separate?

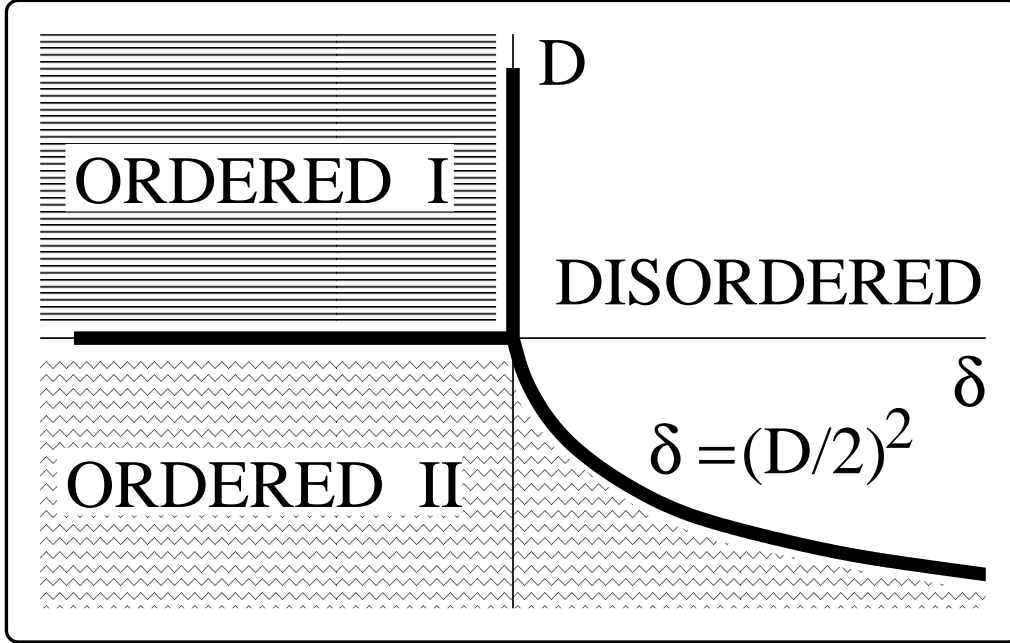


FIG. 1. Schematic phase diagram in the vicinity of a Lifshitz point. The ordered phase I corresponds to ordering at the wave vector $q = 0$ and is shaded by horizontal lines, whereas the ordered phase II corresponds to ordering at $q = \pm\sqrt{-D/2}$ at $D < 0$ and is marked by zig-zag shading.

V. THE PHASE DIAGRAM

To answer this question, one has to recall that, as mentioned above, Lifshitz point is a tricritical point. Thus, generally, one shall expect to see two different ordered phases and one disordered phase in its vicinity, as illustrated by the following toy-model expression for the free energy F at a finite-temperature Lifshitz point:

$$F \sim \phi \left[\delta + Dq^2 + q^4 \right] \phi. \quad (35)$$

As follows from (35), the region $(D > 0, \delta < 0)$ corresponds to the phase ordered at $q = 0$, whereas in the region $(D < 0, \delta < (D/2)^2)$ one finds ordering at wave vectors $q = \pm\sqrt{-D/2}$. This phase diagram is shown in Fig. 1.

To establish the phase diagram near a quantum Lifshitz point, one shall draw the curves

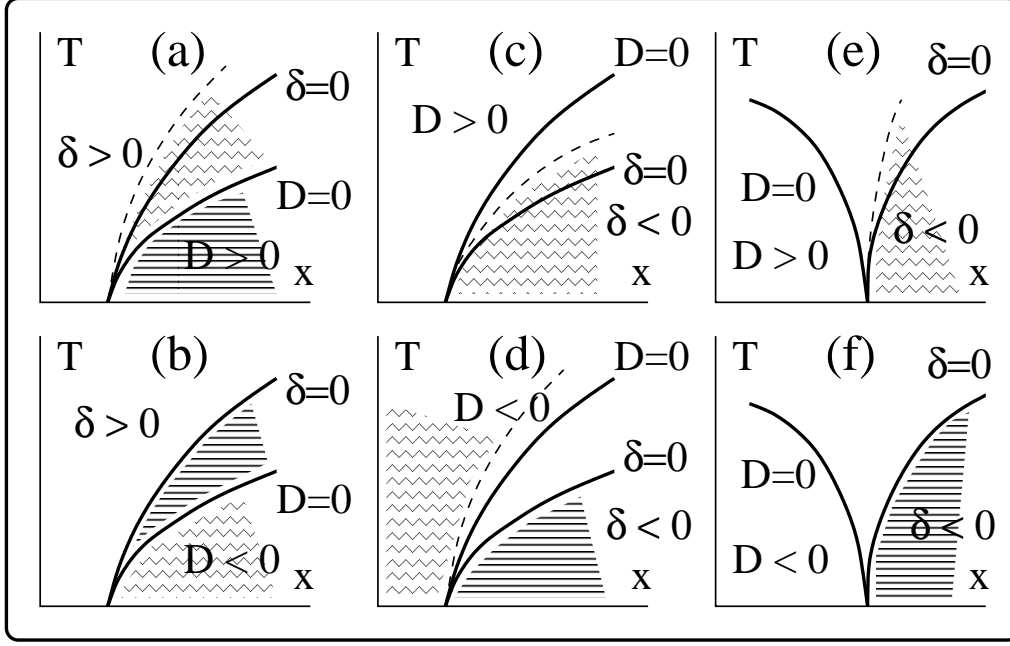


FIG. 2. Schematic phase diagram in the vicinity of a quantum Lifshitz point. As in Fig. 1, horizontal shading denotes “commensurate” ordering (at $q = 0$), whereas zig-zag shading corresponds to “incommensurate” order (at $q = \pm\sqrt{-D/2}$). Wherever shown, dashed line corresponds to $\delta = (D/2)^2$ at $D < 0$. The bold lines defined by $D = 0$ and $\delta = 0$ are determined by equations (30) and (31).

of $\delta(b^*) = 0$ and $D(b^*) = 0$ in the $(T - p)$ plane and compare with Fig. 1. Mutual position of the two curves depends on the relative magnitude of u , v_1 and v_2 , and on the signs of the proportionality coefficients between $r_{1,2}$ and $(p - p_c)$. Six possibilities arise, as shown on Fig. 2. As in Fig. 1, horizontal shading denotes “commensurate” ordering (at $q = 0$), whereas zig-zag shading corresponds to “incommensurate” order (at $q = \pm\sqrt{-D/2}$). Case (d) can be ruled out on physical grounds, as it corresponds to ordering at high temperatures. The possibilities illustrated in Fig. 2 (a) and (b) are irrelevant to the results obtained for CePd_2Si_2 or for $\text{CeCu}_{6-x}\text{Au}_x$, as they lead to existence of two ordered states, whereas no trace of second transition has been found in either of the materials of interest. The remaining cases (c), (e) and (f) are the most interesting for us, as they show how a quantum Lifshitz

point can mimic a “regular” quantum critical point with only one ordered phase. Case (f) corresponds to “commensurate” ordering, while (c) and (e) describe “incommensurate” order. In the latter two cases, the transition line between the “incommensurate” and the disordered phases is described by the equation $\delta(b) = (D(b)/2)^2$, shown in Fig. 2 by dashed line, with $\delta(b)$ and $D(b)$ given by (30-31). At low temperatures, this line asymptotically coincides with the line $\delta(b) = 0$ given by (34).

Currently, the structure of magnetic order in $\text{CeCu}_{6-x}\text{Au}_x$ is being mapped out experimentally by several groups²⁷. However, if a Lifshitz point described above is realized in $\text{CeCu}_{6-x}\text{Au}_x$, the exact character of ordering is irrelevant for the physical properties in the “classical Gaussian” region, roughly corresponding to the vicinity of the line ($T > 0, T_c = 0$).

VI. GENERATION OF STIFFNESS

As shown in Section III (see Fig. 3), near the quantum Lifshitz point the short-range fluctuations do generate stiffness in the “soft” direction, even though it is absent exactly at the critical point. To check the importance of this effect at finite temperature, one has to compare the generated quadratic term Dq_{\perp}^2 with the quartic term q_{\perp}^4 . The comparison can be done easily using the solution (10-14) of the scaling equations (5-9).

At each step of the renormalization procedure, one focuses on momenta and frequencies near the current value of the cut-off. Recalling the agreement to set the cut-off equal to unity, one finds that rescaling factor b corresponds to frequency and momenta $q_{\parallel}(b) = 1/b$, $q_{\perp}(b) = 1/\sqrt{b}$ and $\omega(b) = 1/b^2$.

Thus the relative importance of the generated term $D(b)q_{\perp}^2(b)$ is given by its comparison with the mass term $\delta(b)$ and with the quartic term $q_{\perp}^4(b)$. To do the comparison in the classical Gaussian region which we are studying, one shall set $r_1 = r_2 = 0$ and then, using (10-14), estimate $\delta(b)$ and $D(b)$ at a running value of b .

In the regime of “quantum” renormalization ($T(b) \ll 1$), the sought estimate is given by

$$\delta(b) \sim A(n+2)ub^{-1/2},$$

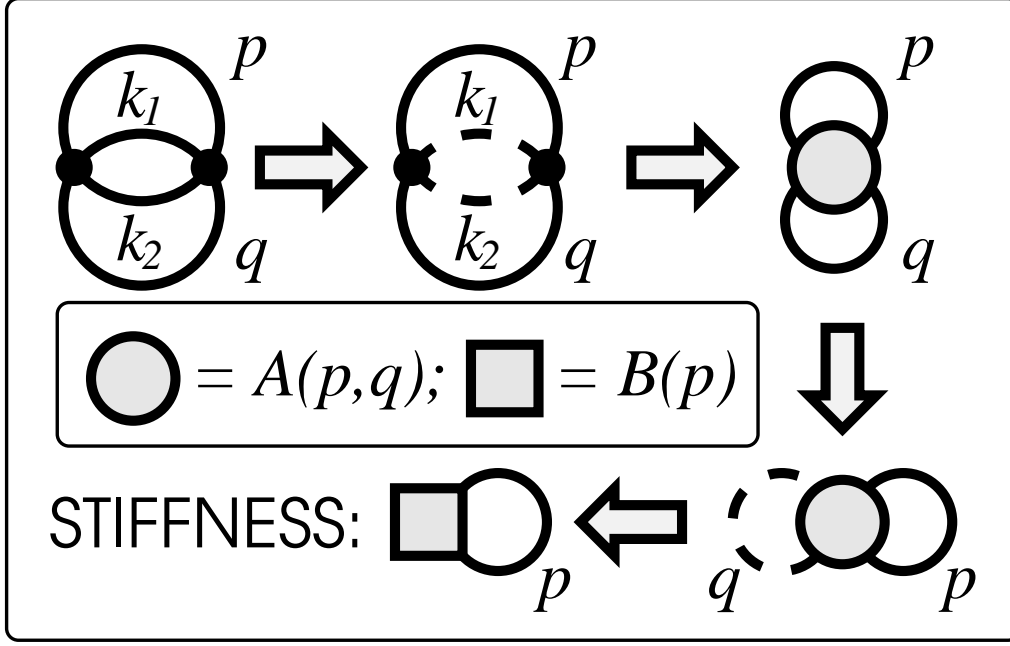


FIG. 3. Generation of stiffness in the “soft” direction by the renormalization process. Propagators of “fast” degrees of freedom, integrated out at each step of renormalization, are shown by dashed lines. The free energy correction in the second order in point-like quartic interaction u (black dot) generates dispersion of the effective quartic interaction (shaded circle). The latter, in turn, gives rise to the stiffness in the “soft” direction (shaded square).

$$D(b) \sim A(nv_1 + v_2)b^{-3/2},$$

$$D(b)q_{\perp}^2(b) \sim A(nv_1 + v_2)b^{-5/2}.$$

$$q_{\perp}^4(b) \sim q_{\parallel}^2(b) \sim |\omega|(b) \sim b^{-2}.$$

Applicability of our scaling equations requires weak coupling ($u, v_{1,2} \ll 1$). Thus, $D(b)q_{\perp}^2(b)$ is negligible compared with $q_{\perp}^4(b)$ at any value of b up to the point when $\delta(b)$ and $q_{\perp}^4(b)$ become of the same order of magnitude. Therefore, the stiffness generated by short-distance fluctuations under the renormalization flow can be safely neglected in our study, which in turn means that the quantum Lifshitz point is well-defined.

VII. CONCLUSIONS

In this paper, I studied the classical Gaussian region near a quantum Lifshitz point. This corresponds to defining the low-temperature behavior at the point where the Néel temperature and the stiffness in the “soft” direction simultaneously become equal to zero. The Néel temperature was found to scale as $T_N \sim (p_c - p)^{4/5}$. The specific heat coefficient was found to have a $T^{1/4}$ anomaly, whereas the resistivity was shown to exhibit $T^{5/4}$ scaling. Of these results, only the resistivity exponent finds experimental support (in CePd_2Si_2 and CeNi_2Ge_2), while the predictions for the shape of the transition line appears to fail in fitting the experimental data. The situation with the specific heat data is not yet entirely certain.

Regardless of possible reasons, discussed briefly in Section II, the failure of simple phenomenology based on the assumption of a quantum Lifshitz point appears to be unambiguous for CePd_2Si_2 and $\text{CeCu}_{6-x}\text{Au}_x$. More generally, it appears that the correct theory of the transition shall fall below the upper critical dimension, while the Hertz-Millis theory and its present refinement are all essentially Gaussian.

At the moment, the source of the puzzling behavior of these Ce-based materials near a zero-temperature transition remains unclear. A comprehensive experimental study (specific heat, neutron scattering, thermal transport and NMR/NQR/ μ SR) might help to resolve some of the pressing issues. An intriguing possible direction of theoretical research would be to study the yet poorly understood interplay between the incipient correlations in the conduction sea and the development of the Kondo effect²⁸.

I am indebted to G. Aeppli, P. Coleman, A. Millis, D. Morr, A. Rosch and A. Schröder for discussions related to this article, and to Y. Aoki and T. Fukuhara for discussions of their data. The work was started at Rutgers University, where it was supported by the National Science Foundation (grant number DMR-96-14999). Work at the University of Illinois was supported in part by the MacArthur Chair endowed by the John D. and Catherine T. MacArthur Foundation at the University of Illinois.

APPENDIX

In this Appendix, I derive the scaling equations (5-9). The first term on the right hand side of each equation corresponds to rescaling of the variable under an infinitesimal time- and length-scale transformation. It can be obtained e.g. by following Hertz³. Rewrite the action (2-4) in the momentum and frequency domain, replacing the sum over the Matsubara frequencies by an integral up to the cut-off (set equal to 1):

$$S_{eff}[\phi] = S^{(2)} + S^{(4)} \quad (36)$$

$$S^{(2)} = \int^1 \frac{d\omega}{2\pi} \int^1 \frac{dq_{\parallel}^2}{(2\pi)^2} \int^1 \frac{dq_{\perp}}{2\pi} \phi_{\alpha} \left[\delta + |\omega| + q_{\parallel}^2 + Dq_{\perp}^2 + q_{\perp}^4 \right] \phi_{\alpha} \quad (37)$$

$$S^{(4)} = \left[\int^1 \frac{d\omega}{2\pi} \int^1 \frac{dq_{\parallel}^2}{(2\pi)^2} \int^1 \frac{dq_{\perp}}{2\pi} \right]_{1,2,3}^3 \left[u(\phi_{\alpha}\phi_{\alpha})^2 + v_1(q_{\perp}\phi_{\alpha})^2\phi_{\beta}\phi_{\beta} + v_2(\phi_{\alpha}q_{\perp}\phi_{\alpha})^2 \right]. \quad (38)$$

Then integrate out a thin shell between the original cut-off (equal to 1) and the new cut-off (equal to $1/b$) in the q_{\parallel} space. Now define thin shells in the ω and q_{\perp} spaces in such a way that upon being integrated out, they would admit rescaling of all the variables ($\omega, q_{\parallel}, q_{\perp}, \delta, D, u, v_1, v_2$ and ϕ_{α}) in such a way as to bring the remaining part of $S^{(2)}$ back exactly to the form (18) with the new values of δ, D, u, v_1 and v_2 . The only choice of rescaling factors which allows this corresponds to rescaling q_{\parallel} by $1/b$, integrating out ω between 1 and $1/b^2$ and rescaling it by $1/b^2$, integrating out q_{\perp} between 1 and $1/\sqrt{b}$ and rescaling it by $1/\sqrt{b}$ – at the expense of rescaling δ and T by b^2 , D by b , u by $1/\sqrt{b}$ and $v_{1,2}$ by $b^{-3/2}$, which corresponds precisely to the first terms on the right hand side of (5-9).

Now, I will obtain the remaining terms in (8-9). First, expand the partition function Z to first order in $S^{(4)}$:

$$Z = Z_0 \left[1 - \langle S^{(4)} \rangle \right].$$

Using Wick's theorem²⁶, the average $\langle S^{(4)} \rangle$ can be conveniently rewritten as

$$\langle S^{(4)} \rangle = n(n+2)u\langle\phi^2\rangle^2 + n(nv_1 + v_2)\langle\phi^2\rangle\langle q_{\perp}^2\phi^2\rangle,$$

where $\langle\phi^2\rangle$ and $\langle q_{\perp}^2\phi^2\rangle$ are defined as per

$$\langle \phi^2 \rangle \equiv \int_0^1 \frac{dz}{\pi} \coth\left(\frac{z}{2T(b)}\right) \int^1 \frac{dq_{\parallel}^2}{(2\pi)^2} \int^1 \frac{dq_{\perp}}{2\pi} \frac{z}{z^2 + [\delta(b) + q_{\parallel}^2 + D(b)q_{\perp}^2 + q_{\perp}^4]^2} \quad (39)$$

$$\langle q_{\perp}^2 \phi^2 \rangle \equiv \int_0^1 \frac{dz}{\pi} \coth\left(\frac{z}{2T(b)}\right) \int^1 \frac{dq_{\parallel}^2}{(2\pi)^2} \int^1 \frac{dq_{\perp}}{2\pi} \frac{z q_{\perp}^2}{z^2 + [\delta(b) + q_{\parallel}^2 + D(b)q_{\perp}^2 + q_{\perp}^4]^2}. \quad (40)$$

The next step amounts to integrating out a thin shell near the cut-off in the expression for $\langle S^{(4)} \rangle$. As described above, such a shell has width $1 - 1/b$ in the q_{\parallel} direction, $1 - 1/b^2$ in the z direction and $1 - 1/\sqrt{b}$ in the q_{\perp} direction. This integration generates the sought terms in (8-9), with

$$\begin{aligned} f_1[T(b), \delta(b), D(b)] &= \frac{1}{2\pi} \int_0^1 \frac{dz}{\pi} \coth\left(\frac{z}{2T(b)}\right) \int^1 \frac{dq_{\perp}}{2\pi} \frac{z}{z^2 + [\delta(b) + 1 + D(b)q_{\perp}^2 + q_{\perp}^4]^2} \\ &+ \frac{2}{\pi} \coth\left(\frac{1}{2T(b)}\right) \int^1 \frac{dq_{\parallel}^2}{(2\pi)^2} \int^1 \frac{dq_{\perp}}{2\pi} \frac{1}{1 + [\delta(b) + q_{\parallel}^2 + D(b)q_{\perp}^2 + q_{\perp}^4]^2} \\ &+ \frac{1}{4\pi} \int_0^1 \frac{dz}{\pi} \coth\left(\frac{z}{2T(b)}\right) \int^1 \frac{dq_{\parallel}^2}{(2\pi)^2} \frac{z}{z^2 + [\delta(b) + q_{\parallel}^2 + D(b) + 1]^2}, \end{aligned} \quad (41)$$

$$\begin{aligned} f_2[T(b), \delta(b), D(b)] &= \frac{1}{2\pi} \int_0^1 \frac{dz}{\pi} \coth\left(\frac{z}{2T(b)}\right) \int^1 \frac{dq_{\perp}}{2\pi} \frac{z}{z^2 + [\delta(b) + 1 + D(b)q_{\perp}^2 + q_{\perp}^4]^2} \\ &+ \frac{2}{\pi} \coth\left(\frac{1}{2T(b)}\right) \int^1 \frac{dq_{\parallel}^2}{(2\pi)^2} \int^1 \frac{dq_{\perp}}{2\pi} \frac{q_{\parallel}^2}{1 + [\delta(b) + q_{\parallel}^2 + D(b)q_{\perp}^2 + q_{\perp}^4]^2} \\ &+ \frac{1}{4\pi} \int_0^1 \frac{dz}{\pi} \coth\left(\frac{z}{2T(b)}\right) \int^1 \frac{dq_{\parallel}^2}{(2\pi)^2} \frac{z q_{\parallel}^2}{z^2 + [\delta(b) + q_{\parallel}^2 + D(b) + 1]^2}, \end{aligned} \quad (42)$$

thus completing the derivation of the scaling equations (8-9).

REFERENCES

- ¹ see e.g. J. Phys.: Cond. Mat. **8**, (1996), or Z. Phys. **B** 103 (1997), for some of the recent references.
- ² L. D. Landau, Sov. Phys. JETP **3**, 920 (1956); Sov. Phys. JETP **8**, 70 (1959).
- ³ J. A. Hertz, Phys. Rev. **B** **14**, 1165 (1976).
- ⁴ A. J. Millis, Phys. Rev. **B** **48**, 7183 (1993).
- ⁵ J. Mathon, Proc. Roy. Soc., **A** **306**, 355 (1968).
- ⁶ K. Makoshi, T. Moriya, J. Phys. Soc. Japan, **38**, 10 (1975).
- ⁷ K. Ueda, J. Phys. Soc. Japan, **43**, 1497 (1977).
- ⁸ I. E. Dzyaloshinskii and P. S. Kondratenko, Sov. Phys. JETP **43**, 1036 (1976).
- ⁹ T. Moriya, *Spin Fluctuations in Itinerant electron Magnetism*, Springer-Verlag, Berlin (1985).
- ¹⁰ for some of the recent references, see M. A. Continentino, preprint cond-mat/9802041.
- ¹¹ S. Ogawa, J. Phys. Soc. Japan, **40**, 1007 (1976); Physica **91 B**, 82 (1977).
- ¹² S. R. Julian *et al.*, Journ. Phys.: Cond. Matt. **8**, 9675 (1996).
- ¹³ H. von Löhneysen, Journ. Phys.: Cond. Matt. **8**, 9689 (1996).
- ¹⁴ A. Schröder *et al.*, Phys. Rev. Lett. **80**, 5623 (1998); preprint cond-mat/9803004.
- ¹⁵ A. Rosch *et al.*, Phys. Rev. Lett. **79**, 159 (1997); preprint cond-mat/9701109.
- ¹⁶ O. Stockert *et al.*, Phys. Rev. Lett. **80**, 5627 (1998); preprint cond-mat/9802086.
- ¹⁷ F. M. Grosche *et al.*, APS e-print server preprint aps1997aug27_001.
- ¹⁸ N. D. Mathur *et al.*, Nature **394**, 39 (1998).

- ¹⁹ see, e.g., P.M. Chaikin and T.C. Lubensky, “Principles of condensed matter physics”, p. 184, Cambridge University Press (1995).
- ²⁰ F. Steglich *et al.*, Journ. Phys.: Cond. Matt. **8**, 9909 (1996); Z. Phys. **B** 103, 235 (1997).
- ²¹ T. Fukuhara *et al.*, Journ. of Magnetism and Magn. Materials **140-144**, 889 (1995).
- ²² Yuji Aoki *et al.*, Journ. Phys. Soc. Jpn. **66**, 2993 (1997); preprint cond-mat/9709229.
- ²³ C. Lacroix *et al.*, Phys. Rev. **B** **54**, 15178 (1996).
- ²⁴ Phys. Rev. Lett. **76**, 2125 (1996).
- ²⁵ A. Rosch, preprint cond-mat/9810260.
- ²⁶ John Cardy, *Scaling and Renormalization in Statistical Physics*, Cambridge University Press (1996).
- ²⁷ A. Schröder and O. Stockert, private communications.
- ²⁸ A. I. Larkin and V. I. Melnikov, Sov. Phys. JETP **34**, 656 (1972).